
Article:
Tian, Y. orcid.org/0000-0003-1772-8850, Gao, X., Liu, W. orcid.org/0000-0003-2968-2888 et al. (2 more authors) (2023) Localization of mixed coherently and incoherently distributed sources based on generalized array manifold. Signal Processing. 109038. ISSN 0165-1684

https://doi.org/10.1016/j.sigpro.2023.109038

Localization of mixed coherently and incoherently distributed sources based on generalized array manifold

Ye Tian[a], Xinyu Gao[b], Wei Liu[c], Hua Chen[a] and Ming Jin[a]

[a] *Faculty of Electrical Engineering and Computer Science, Ningbo University, Ningbo 315211, China*
[b] *School of Information Science and Engineering, Yanshan University, Qinhuangdao 066004, China*
[c] *Department of Electronic and Electrical Engineering, University of Sheffield, Sheffield S1 3JD, U.K.*

Abstract

In practice, signals received by an array may be a mixture of coherently distributed (CD) and incoherently distributed (ID) sources, due to some complicated multipath/scattering effects. To localize mixed CD and ID sources, a method based on the generalized array manifold (GAM) is developed in this work. Firstly, source enumeration and source type classification are achieved by jointly employing the minimum description length (MDL) criterion, the covariance matrix difference technique and the second-order statistics of associated eigenvalues. Secondly, with the source enumeration result, the nominal direction of arrival (DOA) of ID sources is estimated by the rank-reduction principle based one-dimensional (1-D) spectral search, where shift invariance of the GAM associated with ID sources is considered. Thirdly, the oblique projection technique is adopted to separate the CD sources from ID ones, and then the nominal DOA of CD sources is estimated via the sparsity-cognizant total least-squares (S-TLS) method. Finally, with aid of the nominal DOA estimates, the corresponding angular spreads are calculated. An analysis of the proposed method is discussed and the approximate Cramér-Rao bound (CRB) is derived. Simulations are provided to demonstrate the performance of the proposed method.

Keywords: Antenna arrays, mixed source localization, coherently distributed (CD) sources, incoherently distributed (ID) sources.

1. Introduction

Source localization or direction of arrival (DOA) estimation for user terminals (UTs) is a key problem in wireless communications, radar, sonar, radio astronomy and seismic exploration [1], [2]. To tackle

the problem, many methods have been proposed in recent years, such as the multiple signal classification (MUSIC)-based method [3], the estimating signal parameters via rotational invariance technique (ESPRIT)-based method [4] and the sparse recovery based method [5], etc. However, they are mainly focused on the point source model, whose fundamental assumption is that the source signal arrives at the array through one single path and the energy of each source is concentrated to a single direction of the array.

However, in wireless communication systems, the multipath phenomenon caused by reflection and scattering always exists. Hence, the distributed source model which can characterize the impacts of multipath is more appropriate [6], [7]. In general, the distributed sources can be classified into two types: coherently distributed (CD) sources and incoherently distributed (ID) sources, which correspond to slowly time-varying and rapidly time-varying channels, respectively. For a CD source, the signal components arriving from different angles within the extension width are coherent (fully correlated). While for an ID source, these components are uncorrelated. A number of methods focusing on the localization of pure CD or pure ID sources have been presented [8]-[28], and most of them are established on the well-known subspace framework. These activities can be summarized as follows:

1) For pure CD sources, the signal components from different paths are completely correlated, and the dimension of the signal subspace is equal to the number of actual sources/UTs, which is the same as in the point source model. Therefore, many traditional subspace-based approaches for point sources can be easily extended to the case of CD sources. In [8] and [9], the distributed signal parameter estimator and the dimension reduction MUSIC (DRNC-MUSIC) estimator were proposed, which are the generalization of the classical MUSIC method; in [10]-[12], the ESPRIT, the unitary ESPRIT and the ESPRIT-Like approaches were presented with closed-form expressions. The propagator method and the beamspace propagator method were developed in [13] and [14], respectively, which provide a simple way for source localization of CD sources. Except for the subspace-based techniques, the beamforming estimator [15] and sparse reconstruction [16], [17] based approaches were also investigated in literature.

2) For pure ID sources, the signal components from different paths are completely uncorrelated, which directly yields that the dimension of the signal subspace is larger than the number of actual sources/UTs, and thus the source localization problem becomes complicated. Instead of exploiting the traditional subspace technique, Meng and Stoica *et al.* developed the quasi-signal/noise subspace technique and further proposed the dispersed signal parameter estimator [18], which provides a suitable way to tackle the problem of ID source localization. Following [18], many extensions have been proposed. The covariance matching estimation method and the weighted subspace fitting method were introduced in [19] and [20], respectively. The search-free Root-MUSIC method was proposed in [21], the ESPRIT and Sequential ESPRIT based methods were proposed in [22]-[24], and the beamspace-based methods were investigated in [25] and [26]. In addition, several ID source localization methods following other theoretical frameworks were also presented, examples including the sparse Bayesian learning based method [27] and the maximum likelihood (ML) based method [28].

Note that all the existing methods mentioned above consider only one type of distributed sources (either ID sources or CD sources) and assume that the distributed source type is known *a priori*. However, in certain scenarios, such as in wireless communications with complex and diverse regional environments, multiple types of sources may coexist [29]-[31]. For instance, in over-the-horizon scattering communications, the radio waves are scattered because of coherent reflection from the stable layer, and the signals received by the array appear in the form of CD sources. While due to scattering of radio waves by the inhomogeneity of the space medium, the received array signals will appear as an ID source. After over-the-horizon transmission, signals received by the array may be a mixture of CD and ID sources. As a result, the performance of the methods developed for one type of sources could degrade substantially. To our best knowledge, little attention has been paid on dealing with this issue. Under such a circumstance, developing an appropriate method to achieve satisfactory DOA estimation under the coexistence of CD and ID sources is of great necessity. Motivated by this, a mixed CD and ID source localization method built on the generalized uniform linear array (ULA) manifold is proposed in this

paper. Different from the existing methods, our method is general, which is not only suitable for pure CD or pure ID sources, but also for mixed CD and ID sources. To be specific, the main contributions of this paper are listed as follows.

- As opposed to existing works for pure CD and pure ID sources, a mixed CD and ID source model based on GAM is considered, which is general and better suited for the actual complicated multipath scenarios. Based on this model, a new solution jointly utilizing the shift invariance of the ID GAM, the oblique projection operator and the sparsity-cognizant total least-squares (S-TLS) method [32] has been developed. It is shown that the shift invariance of the ID GAM combined with the rank deficient principle can yield unambiguous nominal DOA estimation of ID sources. Meanwhile, the oblique projection operator together with the S-TLS method has also been verified to be a more effective way to estimate DOAs of CD sources than some existing methods.

- An efficient source enumeration scheme jointly exploiting the minimum description length (MDL) criterion, the covariance matrix difference technique and the second-order statistics of associated eigenvalues is introduced, which can yield effective estimation of both the number of CD sources and that of ID sources, and hence provides a solid starting point for the subsequent source localization process. To the best of our knowledge, it is the first time to apply such a scheme for source enumeration, and is also an effective solution we developed for estimation of the number of mixed distributed sources.

- An analysis in terms of maximum number of detectable distributed sources, estimation accuracy, computational complexity and capacity for localizing distributed sources in different scenarios is provided. Moreover, an approximate Cramér-Rao bound (CRB) is also derived.

The rest of this paper is organized as follows. In Section **2**, the signal model for mixed CD and ID sources, as well as the major assumptions is provided. In Section **3**, the proposed mixed source localization method is presented in detail. In Section **4**, an analysis of the proposed method is provided,

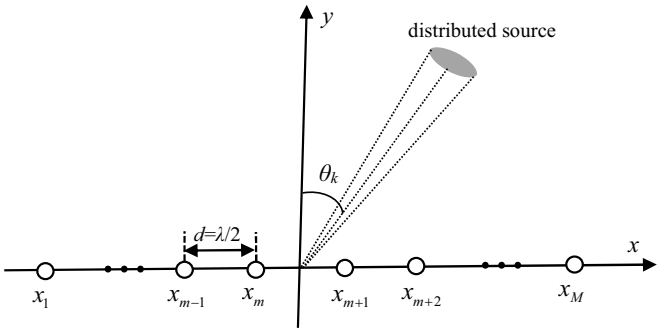

Figure 1: Geometry of the considered uniform linear array.

and the approximate CRB is derived. Simulation results are given in Section **5**, and conclusions are drawn in Section **6**.

Notations: Lowercase (uppercase) boldface symbols represent vectors (matrices). The superscripts $(\cdot)^T$, $(\cdot)^H$, $(\cdot)^*$, $(\cdot)^\dagger$, $(\cdot)^{-1}$ and $(\cdot)^{1/2}$ stand for the transpose, the conjugate transpose, the conjugate, the pseudo-inverse, the inverse and the square root operations, respectively. $\mathbb{E}\{\cdot\}$, diag$\{\cdot\}$, blkdiag$\{\cdot\}$, det$[\cdot]$ and vec$(\cdot)$ denote the statistical expectation, the diagonalization, the block diagonalization, the determinant and the vectorization, respectively. $\otimes$ and $\odot$ are the Kronecker and the Hadamard-Schur products, respectively. $\mathbf{I}_M$ stands for an $M \times M$ identify matrix, $\mathbf{\Pi}_M$ an $M \times M$ exchange matrix, $\lceil\cdot\rceil$ the ceiling operation, and $\delta(\cdot)$ the Kronecker delta function.

2. Mixed CD and ID Signal Model

Suppose that K uncorrelated[1] narrowband sources (containing K_1 ID sources and $K_2 = K - K_1$ CD sources transmitted by UTs) impinge on a ULA with M sensors, as shown in Fig. 1. Let d denote the distance between adjacent sensors, which equals half of the wavelength λ. The received signals by the ULA can be expressed as

$$\mathbf{y}(t) = \mathbf{y}_I(t) + \mathbf{y}_C(t) + \mathbf{n}(t), \tag{1}$$

[1]Uncorrelated signals means that different source signals are uncorrelated, while coherently distributed sources means that the signal components of a source from different paths are coherent.

where $\mathbf{y}_I(t)$ and $\mathbf{y}_C(t)$ correspond to the received data of ID and CD sources at time index t, respectively, and $\mathbf{n}(t)$ is the additive white Gaussian noise with zero-mean and variance σ_n^2.

For ID sources, the received signals $\mathbf{y}_I(t)$ is given by [22]

$$\mathbf{y}_I(t) = \sum_{k=1}^{K_1} s_k(t) \sum_{i=1}^{N_k} \gamma_{k,i}(t)\mathbf{a}(\theta_{k,i}(t)), \tag{2}$$

where $\mathbf{a}(\theta_{k,i}(t)) = [e^{jx_1 u \sin(\theta_{k,i}(t))}, \ldots, e^{jx_M u \sin(\theta_{k,i}(t))}]^T$, $\theta_{k,i}(t) = \theta_k + \tilde{\theta}_{k,i}(t)$ with θ_k and $\tilde{\theta}_{k,i}(t)$ representing the nominal DOA and the angular deviation of the ith path for the kth UT, respectively. In particular, $\tilde{\theta}_{k,i}(t)$ is a real-valued random process with zero mean and standard deviation σ_{θ_k}, which is referred to as the angular spread. $u = -2\pi/\lambda$ and x_m is the coordinate of the mth element; $\gamma_{k,i}(t)$ denotes the complex-valued path gain corresponding to the ith path from the kth UT, and N_k the number of multipaths.

By exploiting the GAM of ID sources and the first-order approximation of Taylor expansion under a small angular spread, $\mathbf{y}_I(t)$ can be approximately written as [22]

$$\mathbf{y}_I(t) \approx \sum_{k=1}^{K_1} [\mathbf{a}(\theta_k)v_{k,0}(t) + \mathbf{d}(\theta_k)v_{k,1}(t)], \tag{3}$$

where $\mathbf{d}(\theta_k) = \partial\mathbf{a}(\theta_k)/\partial\theta_k$, and

$$v_{k,0}(t) = s_k(t) \sum_{i=1}^{N_k} \gamma_{k,i}(t), \tag{4}$$

$$v_{k,1}(t) = s_k(t) \sum_{i=1}^{N_k} \gamma_{k,i}(t)\tilde{\theta}_{k,i}(t). \tag{5}$$

For CD sources, the signal model $\mathbf{y}_C$ is given by [33], [34],

$$\mathbf{y}_C = \sum_{k=K_1+1}^{K} s_k(t) \sum_{i=1}^{N_k} \gamma_{k,i}(t)\mathbf{a}(\theta_{k,i}(t)) = \sum_{k=K_1+1}^{K} \sum_{i=1}^{N_k} \mathbf{a}(\theta_{k,i}(t))s_{k,i}(t), \tag{6}$$

where $s_{k,i}(t)$ stands for the complex amplitude of the ith path from the kth CD source at the receiving array side.

According to the large number theorem, when the number of multipaths N_k of a CD source is large enough, DOA will exhibit continuous distribution within certain spatial range, which implies that $\mathbf{y}_C$

can be expressed as [35]

$$\mathbf{y}_C = \sum_{k=K_1+1}^{K} \int \mathbf{a}(\theta) s_k(\theta, t; \theta_k, \sigma_{\theta_k}) d\theta, \tag{7}$$

where $s_k(\theta, t; \theta_k, \sigma_{\theta_k})$ represents angular signal density of the kth CD source, with θ_k and σ_{θ_k} denoting its nominal DOA and angular spread, respectively. Due to coherence of the signal components of CD sources from different paths, the angular signal density can be represented as [8]-[10]

$$s_k(\theta, t; \theta_k, \sigma_{\theta_k}) = s_k(t) \rho(\theta; \theta_k, \sigma_{\theta_k}) \tag{8}$$

Subsequently, it can be derived that

$$\mathbf{y}_C = \sum_{k=K_1+1}^{K} s_k(t) \mathbf{c}(\theta_k, \sigma_{\theta_k}), \tag{9}$$

where $\mathbf{c}(\theta_k, \sigma_{\theta_k}) = \int \mathbf{a}(\theta_k) \rho(\theta; \theta_k, \sigma_{\theta_k}) d\theta$ denotes the generalized steering vector with $\rho(\theta; \theta_k, \sigma_{\theta_k})$ being the probability density function of the angular spread. With a small angular spread, an approximative expression of $\mathbf{c}(\theta_k, \sigma_{\theta_k})$ is given by

$$\mathbf{c}(\theta_k, \sigma_{\theta_k}) \approx \mathbf{a}(\theta_k) \odot \mathbf{g}(\theta_k, \sigma_{\theta_k}), \tag{10}$$

whose mth element is

$$\begin{aligned} [\mathbf{c}(\theta_k, \sigma_{\theta_k})]_m &\approx \int e^{j x_m u (\sin\theta_k + \tilde{\theta}\cos\theta_k)} \rho(\tilde{\theta}; \theta_k, \sigma_{\theta_k}) d\tilde{\theta} \\ &= e^{j x_m u \sin\theta_k} \int e^{j x_m u \tilde{\theta} \cos\theta_k} \rho(\tilde{\theta}; \theta_k, \sigma_{\theta_k}) d\tilde{\theta} = [\mathbf{a}(\theta_k)]_m [\mathbf{g}(\theta_k, \sigma_{\theta_k})]_m, \end{aligned} \tag{11}$$

where $[\mathbf{a}(\theta_k)]_m = \exp(j x_m u \sin\theta_k)$. In general, $\rho(\theta_k, \sigma_{\theta_k})$ is assumed to be of uniform or Gaussian distribution [8-10]. Thus, it can be further derived that

$$[\mathbf{g}(\theta_k, \sigma_{\theta_k})]_m = \begin{cases} \frac{\sin(x_m \sigma_{\theta_k}/d)}{x_m \sigma_{\theta_k}/d}, & \text{uniform,} \\ e^{-(x_m \sigma_{\theta_k}/d)^2/2}, & \text{Gaussian.} \end{cases} \tag{12}$$

In matrix form, (1) becomes

$$\mathbf{y}(t) \approx \mathbf{A}\mathbf{S}_{I_1}(t) + \mathbf{B}\mathbf{S}_{I_2}(t) + \mathbf{C}\mathbf{S}_C(t) + \mathbf{n}(t) = \mathbf{D}\mathbf{V}(t) + \mathbf{n}(t), \tag{13}$$

where $\mathbf{D} = [\mathbf{A}, \mathbf{B}, \mathbf{C}]$, $\mathbf{V}(t) = [\mathbf{S}_{I_1}(t), \mathbf{S}_{I_2}(t), \mathbf{S}_C(t)]^T$, and

$$\mathbf{A} = [\mathbf{a}(\theta_1), \ldots, \mathbf{a}(\theta_{K_1})], \mathbf{B} = [\mathbf{d}(\theta_1), \ldots, \mathbf{d}(\theta_{K_1})], \tag{14}$$

$$\mathbf{C} = [\mathbf{c}(\theta_{K_1+1}, \sigma_{\theta_{K_1+1}}), \ldots, \mathbf{c}(\theta_K, \sigma_{\theta_K})], \tag{15}$$

$$\mathbf{S}_{I_1}(t) = [v_{1,0}(t), v_{2,0}(t), \ldots, v_{K_1,0}(t)]^T, \tag{16}$$

$$\mathbf{S}_{I_2}(t) = [v_{1,1}(t), v_{2,1}(t), \ldots, v_{K_1,1}(t)]^T, \tag{17}$$

$$\mathbf{S}_C(t) = [\mathbf{s}_{K_1+1}, \mathbf{s}_{K_1+2}, \ldots, \mathbf{s}_K(t)]^T. \tag{18}$$

Throughout the paper, we make the following assumptions:

- The angular deviation $\tilde{\theta}_{k,i}(t)$ and the complex-valued gain $\gamma_{k,i}(t)$ are temporally white and independent with zero-mean and covariance

$$\mathbb{E}\{\tilde{\theta}_{k,i}(t)\tilde{\theta}_{\tilde{k},\tilde{i}}(\tilde{t})\} = \sigma^2_{\theta_k}\delta(k-\tilde{k})\delta(i-\tilde{i})\delta(t-\tilde{t}), \tag{19}$$

$$\mathbb{E}\{\gamma_{k,i}(t)\gamma^*{}_{\tilde{k},\tilde{i}}(\tilde{t})\} = \frac{\sigma^2_{\gamma_k}}{N_k}\delta(k-\tilde{k})\delta(i-\tilde{i})\delta(t-\tilde{t}). \tag{20}$$

- The UTs are located in a small angle scattering environment, i.e., the angular spreads $\{\sigma_{\theta_k}\}_{k=1}^K$ are rather small.

- The signals are uncorrelated, and narrowband with zero mean and covariance $\mathbb{E}\{\mathbf{s}(t)\mathbf{s}^H(t)\} = \mathrm{diag}\{p_1, \ldots, p_K\}$, where p_k is the power of the kth signal.

- The transmitted signals, angular deviations, path gains and noise are mutually uncorrelated.

- The number of UTs K satisfies $K \leq \lceil M/2 \rceil - 2$, and the number of multipaths N_k is large, $\forall k \in [1, K]$.

Based on (13) and the above assumptions, the array covariance matrix can be expressed as

$$\begin{aligned}\mathbf{R} &= \mathbb{E}\{\mathbf{y}(t)\mathbf{y}^H(t)\} = \mathbf{D}\mathbf{\Lambda}\mathbf{D}^H + \sigma_n^2\mathbf{I}_M \\ &= \mathbf{A}\mathbf{\Lambda}_{I_1}\mathbf{A}^H + \mathbf{B}\mathbf{\Lambda}_{I_2}\mathbf{B}^H + \mathbf{C}\mathbf{\Lambda}_C\mathbf{C}^H + \sigma_n^2\mathbf{I}_M,\end{aligned} \tag{21}$$

where

$$\mathbf{\Lambda} = \text{blkdiag}\{\mathbf{\Lambda}_{I_1}, \mathbf{\Lambda}_{I_2}, \mathbf{\Lambda}_C\}, \tag{22}$$

$$\mathbf{\Lambda}_{I_1} = \text{diag}\{P_1, \ldots, P_{K_1}\}, \tag{23}$$

$$\mathbf{\Lambda}_{I_2} = \text{diag}\{P_1\sigma_{\theta_1}^2, \ldots, P_{K_1}\sigma_{\theta_{K_1}}^2\}, \tag{24}$$

$$\mathbf{\Lambda}_C = \text{diag}\{p_{K_1+1}, \ldots, p_K\}, \tag{25}$$

and $P_k = \sigma_{\gamma_k}^2 p_k, k = 1, \ldots, K_1$. In case of N samples, $\mathbf{R}$ is normally calculated by $\hat{\mathbf{R}} = \frac{1}{N}\sum_{t=1}^{N}\mathbf{y}(t)\mathbf{y}^H(t)$. In the following, we demonstrate how to utilize $\hat{\mathbf{R}}$ to achieve mixed CD and ID sources localization.

3. Proposed Method

3.1. Source Enumeration

Estimation of the number of sources where ID and CD sources coexist is required prior to performing DOA estimation. Based on the MDL criterion [36], the number of sources can be estimated by

$$\hat{\bar{K}} = \arg\min_{\bar{K}}(M-\bar{K})N\log\left[\frac{\frac{1}{M-\bar{K}}\sum_{i=\bar{K}+1}^{M}\hat{l}_i}{\prod_{i=\bar{K}+1}^{M}\hat{l}_i^{\frac{1}{M-\bar{K}}}}\right] + v_{\bar{K}}, \tag{26}$$

where $\bar{K}$ is the assumed number of sources, $v_{\bar{K}} = \frac{1}{2}\bar{K}(2M-\bar{K})\log N$ with N denoting the number of samples, $\hat{l}_1, \ldots, \hat{l}_M$ are eigenvalues in descending order of the sampled covariance matrix $\hat{\mathbf{R}}$. It can be seen from (13) and (21) that the GAM can be regarded as a virtual point source model composed of $2K_1 + K_2$ sources, due to the scattering characteristic of ID sources. As it has been widely demonstrated in literature that MDL is an effective criterion for source enumeration using the point source model, it has been adopted here, and when $\hat{\bar{K}}$ is correctly detected, it will be equal to $2K_1 + K_2$, which is larger than the actual number of sources K. Therefore, we here designate $\hat{\bar{K}}$ as the virtual number of sources.

Next, the covariance difference technique and the second-order statistics of associated eigenvalues are exploited to further obtain the estimation of actual number of ID and CD sources. The covariance difference technique is an efficient tool for distinguishing two covariance matrices that hold different

structures, and has been applied in the localization of uncorrelated and coherent signals [37], DOA estimation in Toeplitz colored noise [38], and classification of mixed far-field and near-field sources [39], etc. However, to the best of our knowledge, it is the first time to apply it for source enumeration, and is also an effective solution we developed for estimation of the number of mixed distributed sources. For ULA, it can be observed that $\mathbf{R}_1 = \mathbf{A}\mathbf{\Lambda}_{I_1}\mathbf{A}^H$ and the noise covariance matrix has a Hermitian Toeplitx structure, while $\mathbf{R}_2 = \mathbf{B}\mathbf{\Lambda}_{I_2}\mathbf{B}^H$ and $\mathbf{R}_3 = \mathbf{C}\mathbf{\Lambda}_C\mathbf{C}^H$ are only Hermitian, which provides a feasible way to eliminate the information of ID sources according to the difference in matrix structure. For the Toeplitz matrix, we have

$$\mathbf{R}_1 = \mathbf{\Pi}_M\mathbf{R}_1^T\mathbf{\Pi}_M, \tag{27}$$

$$\sigma_n^2\mathbf{I}_M = \mathbf{\Pi}_M(\sigma_n^2\mathbf{I}_M)^T\mathbf{\Pi}_M, \tag{28}$$

which directly yields that the covariance difference matrix $\mathbf{R}_D$ can be expressed as

$$\begin{aligned}\mathbf{R}_D &= \mathbf{R} - \mathbf{\Pi}_M\mathbf{R}^T\mathbf{\Pi}_M \\ &= \mathbf{R}_2 - \mathbf{\Pi}_M\mathbf{R}_2^T\mathbf{\Pi}_M + \mathbf{R}_3 - \mathbf{\Pi}_M\mathbf{R}_3^T\mathbf{\Pi}_M.\end{aligned} \tag{29}$$

Since $\mathbf{R}_2^T = \mathbf{R}_2^*$ and $\mathbf{R}_3^T = \mathbf{R}_3^*$, $\mathbf{R}_D$ can be rewritten as

$$\mathbf{R}_D = \mathbf{B}_D\bar{\mathbf{\Lambda}}_{I_2}\mathbf{B}_D^H + \mathbf{C}_D\bar{\mathbf{\Lambda}}_C\mathbf{C}_D^H, \tag{30}$$

where $\mathbf{B}_D = (\mathbf{B}, \mathbf{\Pi}_M\mathbf{B}^*), \mathbf{C}_D = (\mathbf{C}, \mathbf{\Pi}_M\mathbf{C}^*)$, $\bar{\mathbf{\Lambda}}_{I_2} = \text{blkdiag}\{\mathbf{\Lambda}_{I_2}, -\mathbf{\Lambda}_{I_2}\}$, and $\bar{\mathbf{\Lambda}}_C = \text{blkdiag}\{\mathbf{\Lambda}_C, -\mathbf{\Lambda}_C\}$. It can be found that there is neither any component of $\mathbf{R}_1$ nor sensor noise in $\mathbf{R}_D$.

Performing eigenvalue decomposition (EVD) on $\mathbf{R}_D$ yields

$$\mathbf{R}_D = \mathbf{U}\mathbf{\Sigma}\mathbf{U}^H = \sum_{i=1}^{M} l_i\mathbf{u}_i\mathbf{u}_i^H, \tag{31}$$

where $\mathbf{U} = [\mathbf{u}_1, \ldots, \mathbf{u}_M]$ and $\mathbf{\Sigma} = \text{diag}\{l_1, \ldots, l_M\}$ with $l_1 \geq \cdots \geq l_K > l_{K+1} = \cdots l_{M-K} = 0 > l_{M-K+1} \geq \cdots \geq l_M$. If l_i is an eigenvalue of $\mathbf{R}_D$, i.e.,

$$\mathbf{R}_D\mathbf{u}_i = [\mathbf{R} - \mathbf{\Pi}_M\mathbf{R}^T\mathbf{\Pi}_M]\mathbf{u}_i = l_i\mathbf{u}_i, \tag{32}$$

then

$$\mathbf{\Pi}_M[\mathbf{\Pi}_M\mathbf{R}\mathbf{\Pi}_M - \mathbf{R}^T]\mathbf{\Pi}_M\mathbf{u}_i = l_i\mathbf{u}_i. \tag{33}$$

Based on the properties of $\mathbf{\Pi}_M\mathbf{\Pi}_M = \mathbf{I}_M$ and $\mathbf{R}^* = \mathbf{R}^T$, it can be obtained that

$$\mathbf{R}_D\mathbf{\Pi}_M\mathbf{u}_i^* = [\mathbf{R} - \mathbf{\Pi}_M\mathbf{R}^T\mathbf{\Pi}_M]\mathbf{\Pi}_M\mathbf{u}_i^* = -l_i\mathbf{\Pi}_M\mathbf{u}_i^*, \tag{34}$$

which implies that the eigenvalues of $\mathbf{R}_D$ will appear symmetrically, i.e., $l_1 = -l_M, \cdots, l_K = -l_{M-K+1}$. For the sake of simplicity, only the first $\bar{M} = \lceil M/2 \rceil$ eigenvalues are utilized for source enumeration.

Define $\Delta l_i = l_i - l_{i+1}(i = 1, \ldots, \bar{M} - 1)$, whose corresponding second-order statistics β_i is given by

$$\beta_k = \frac{1}{\bar{M} - k}\sum_{i=k}^{\bar{M}-1}\left[\Delta l_i - \frac{1}{\bar{M} - k}\sum_{j=k}^{\bar{M}-1}\Delta l_j\right]^2, \tag{35}$$

where $k = 1, \ldots, \bar{M} - 1$. With β_k, we further construct the decision function for source enumeration as

$$T(k) = \begin{cases} \frac{\beta_{k+1}}{\beta_k}, \beta_k > 0, \\ +\infty, \beta_k = 0. \end{cases} \tag{36}$$

According to (36) and the properties of eigenvalues of $\mathbf{R}_D$, it can be obtained that $T(k)$ satisfies

$$T(k) = \begin{cases} c > 0, k = 1, \ldots, K - 1, \\ 0, \quad k = K, \\ +\infty, \ k = K + 1, \ldots, \bar{M} - 2. \end{cases} \tag{37}$$

Subsequently, the number of sources K is estimated by

$$\hat{K} = \underset{k=1,\ldots,\bar{M}-2}{\arg\min}\ \{T(k)\}. \tag{38}$$

With the estimated $\hat{\bar{K}}$ and $\hat{K}$, the number of ID sources K_1 and CD sources K_2 are finally estimated as

$$\hat{K}_1 = \hat{\bar{K}} - \hat{K}, \ \ \hat{K}_2 = 2\hat{K} - \hat{\bar{K}}. \tag{39}$$

For clarification, the scheme is summarized in Algorithm 1, where $\hat{\chi}$ denotes the estimate of χ with N samples.

Algorithm 1 Source Enumeration of Mixed ID and CD Sources

1: Calculate the covariance matrix $\hat{\mathbf{R}} = \frac{1}{N}\sum_{t=1}^{N}\mathbf{y}(t)\mathbf{y}^H(t)$.

2: Estimate the virtual number of sources $\hat{\bar{K}}$ by the MDL criterion via (26).

3: Construct the covariance difference matrix $\hat{\mathbf{R}}_D$ via $\hat{\mathbf{R}}_D = \hat{\mathbf{R}} - \mathbf{\Pi}_M\hat{\mathbf{R}}\mathbf{\Pi}_M$.

4: Perform EVD on $\hat{\mathbf{R}}_D$ to obtain M eigenvalues, and then choose the first $\bar{M}$ elements after placing them in a descending order.

5: Calculate $\Delta\hat{l}_i = \hat{l}_i - \hat{l}_{i+1}, i = 1,\ldots,\bar{M}-1$, and $\hat{\beta}_k$ by $\hat{\beta}_k = \frac{1}{\bar{M}-k}\sum\limits_{i=k}^{\bar{M}-1}\left[\Delta\hat{l}_i - \frac{1}{\bar{M}-k}\sum\limits_{j=k}^{\bar{M}-1}\Delta\hat{l}_i\right]^2, k = 1,\ldots,\bar{M}-2$.

6: Construct the decision function $\hat{T}(k)$, and further obtain the estimation of K by $\hat{K} = \underset{k=1,\ldots,\bar{M}-2}{\arg\min}\{\hat{T}(k)\}$.

7: Obtain the number of sources estimation of ID and CD sources through (39).

3.2. Nominal DOA Estimation of ID Sources

With the estimation result of the number of sources, we now focus on the nominal DOA estimation of ID sources. In detail, we divide the whole array into two overlapped subarrays with equal number of sensors. Subarray1 contains the first $M-1$ sensors, while subarray2 contains the last $M-1$ sensors. Under this division, the GAMs of these two subarrays are given by

$$\mathbf{D}_1 = [\mathbf{A}_1, \mathbf{B}_1, \mathbf{C}_1],\ \mathbf{D}_2 = [\mathbf{A}_2, \mathbf{B}_2, \mathbf{C}_2], \tag{40}$$

where

$$\mathbf{A}_n = [\mathbf{a}_n(\theta_1),\ldots,\mathbf{a}_n(\theta_{K_1})], \mathbf{B}_n = [\mathbf{d}_n(\theta_1),\ldots,\mathbf{d}_n(\theta_{K_1})],$$

$$\mathbf{C}_n = [\mathbf{c}_n(\theta_{K_1+1}, \sigma_{\theta_{K_1+1}}),\ldots,\mathbf{c}_n(\theta_K, \sigma_{\theta_K})], n = 1, 2.$$

It can be seen that

$$\mathbf{a}_2(\theta_k) = \mathbf{\Phi}_{k1}\mathbf{a}_1(\theta_k),\ \ \mathbf{d}_2(\theta_k) = \mathbf{\Phi}_{k2}\mathbf{d}_1(\theta_k), \tag{41}$$

where

$$\mathbf{\Phi}_{k1} = \mathrm{diag}\left\{e^{jdu\sin\theta_k},\ldots,e^{jdu\sin\theta_k}\right\}, \tag{42}$$

$$\mathbf{\Phi}_{k2} = \text{diag}\left\{\frac{x_2}{x_1}e^{jdu\sin\theta_k}, \ldots, \frac{x_M}{x_{M-1}}e^{jdu\sin\theta_k}\right\}. \tag{43}$$

Meanwhile, with a small angular spread, $\mathbf{c}_2(\theta_k, \sigma_{\theta_k})$ will be approximate to $\mathbf{\Phi}_{k1}\mathbf{c}_1(\theta_k, \sigma_{\theta_k})$. In what follows, the relationship between $\mathbf{d}_1(\theta)$ and $\mathbf{d}_2(\theta)$ is exploited for nominal DOA estimation of ID sources.

Based on estimation result of the number of sources, we implement EVD on $\mathbf{R}$ to yield

$$\mathbf{R} = \mathbf{E}_s\mathbf{\Sigma}_s\mathbf{E}_s^H + \mathbf{E}_n\mathbf{\Sigma}_n\mathbf{E}_n^H, \tag{44}$$

where $\mathbf{\Sigma}_s$ and $\mathbf{\Sigma}_n$ are the diagonal matrices with the largest $K + K_1$ and the remaining $M - K - K_1$ eigenvalues, respectively. $\mathbf{E}_s$ and $\mathbf{E}_n$ are the corresponding $M \times (K + K_1)$ -dimensional signal subspace and $M \times (M - K - K_1)$-dimensional noise subspace, respectively.

$\mathbf{E}_s$ can be partitioned as

$$\mathbf{E}_s = \begin{bmatrix} \mathbf{E}_{s1} \\ \mathbf{d}_M\mathbf{T} \end{bmatrix} = \begin{bmatrix} \mathbf{d}_1\mathbf{T} \\ \mathbf{E}_{s2} \end{bmatrix}, \tag{45}$$

which satisfies $\mathbf{E}_s = \mathbf{D}\mathbf{T}$, $\mathbf{E}_{s1} = \mathbf{D}_1\mathbf{T}$ and $\mathbf{E}_{s2} = \mathbf{D}_2\mathbf{T}$, where $\mathbf{T}$ is an invertible $(K + K_1) \times (K + K_1)$ matrix, $\mathbf{d}_M$ and $\mathbf{d}_1$ stand for the last row and first row of $\mathbf{D}$, respectively.

With $\mathbf{E}_{s1}$ and $\mathbf{E}_{s2}$, further define a new matrix as

$$\mathbf{\Xi}(\theta) = \mathbf{E}_{s2} - \mathbf{\Psi}(\theta)\mathbf{E}_{s1} = (\mathbf{D}_2 - \mathbf{\Psi}(\theta)\mathbf{D}_1)\mathbf{T} = \mathbf{P}\mathbf{T}, \tag{46}$$

where

$$\mathbf{\Psi}(\theta) = \text{diag}\left\{\frac{x_2}{x_1}e^{jdu\sin\theta}, \ldots, \frac{x_M}{x_{M-1}}e^{jdu\sin\theta}\right\}, \tag{47}$$

and the kth column $\mathbf{p}_{ak}(\theta)$, the $(k+K_1)$th column $\mathbf{p}_{dk}$ $(k \in [1, K_1])$, and the $(\bar{k}+2K_1)$th column $\mathbf{p}_{c\bar{k}}(\theta)$ $(\bar{k} \in [1, K - K_1])$ of $\mathbf{P}$ are respectively given by

$$\mathbf{p}_{ak}(\theta) = [\Phi_{k1} - \mathbf{\Psi}(\theta)]\mathbf{a}_1(\theta_k), \tag{48}$$

$$\mathbf{p}_{dk}(\theta) = [\Phi_{k2} - \mathbf{\Psi}(\theta)]\mathbf{d}_1(\theta_k), \tag{49}$$

$$\mathbf{p}_{ck}(\theta, \sigma_\theta) = \mathbf{c}_2(\theta, \sigma_\theta) - \mathbf{\Psi}(\theta)\mathbf{c}_1(\theta, \sigma_\theta). \tag{50}$$

It can be seen that only $\mathbf{p}_{dk}(\theta)$ will be zero when $\theta = \theta_k$, since $\mathbf{\Psi}(\theta_k) = \mathbf{\Phi}_{k2}$ for $k = 1, \ldots, K_1$, which implies that $\mathbf{\Xi}(\theta)$ is rank deficient and the determinant of $\mathbf{\Xi}^H(\theta)\mathbf{\Xi}(\theta))$ is zero, provided that $\theta = \theta_k$ and $K + K_1 \leq M$. Further notice that the above rank-deficiency feature no longer holds for nominal DOA of CD sources, which means that we can achieve unambiguous nominal DOA estimation of ID sources $\{\hat{\theta}_k\}_{k=1}^{K_1}$ by finding K_1 peaks of the following spatial spectral function

$$\eta_I(\theta) = \max_{\theta} \{\det[\mathbf{\Xi}^H(\theta)\mathbf{\Xi}(\theta)]\}^{-1}. \tag{51}$$

3.3. Nominal DOA Estimation of CD sources

To classify mixed ID and CD sources efficiently and further achieve a good DOA estimation of CD sources, the oblique projection technique [40]-[42] is exploited here. Specifically, with the DOA estimates of ID sources $\{\hat{\theta}_k, k = 1, \ldots, K_1\}$, the ID array manifold matrix can be estimated by

$$\mathbf{\Gamma} = [\hat{\mathbf{A}}, \hat{\mathbf{B}}] = [\mathbf{a}(\hat{\theta}_1), \ldots, \mathbf{a}(\hat{\theta}_{K_1}), \mathbf{d}(\hat{\theta}_1), \ldots \mathbf{d}(\hat{\theta}_{K_1})]. \tag{52}$$

Let $\mathbf{E}_{op} = \mathbf{\Gamma}(\mathbf{\Gamma}^H\mathbf{R}^\dagger\mathbf{\Gamma})^{-1}\mathbf{\Gamma}^H\mathbf{R}^\dagger$ be an oblique projection matrix with range space $\mathbf{\Gamma}$ and null space $\mathbf{C}$, which has the following properties

$$\mathbf{E}_{op}\mathbf{\Gamma} = \mathbf{\Gamma}, \quad \mathbf{E}_{op}\mathbf{C} = \mathbf{0}. \tag{53}$$

Then, we apply $\mathbf{E}_{op}$ to $\mathbf{y}(t)$ as follows

$$\mathbf{z}(t) = (\mathbf{I}_M - \mathbf{E}_{op})\mathbf{y}(t) = \mathbf{C}\mathbf{S}_C(t) + (\mathbf{I}_M - \mathbf{E}_{op})\mathbf{n}(t). \tag{54}$$

It can be seen from (54) that the signal part of $\mathbf{z}(t)$ only contains the information of CD sources, whose covariance matrix is $\mathbf{R}_z = \mathbb{E}\{\mathbf{z}(t)\mathbf{z}^H(t)\}$. To achieve satisfied nominal DOA estimation of CD sources, the S-TLS method is exploited here, which not only holds the advantage of super resolution, but also robustness to noise and small perturbations.

By subtracting noise component from $\mathbf{R}_z$, we have

$$\bar{\mathbf{R}}_z = \mathbf{R}_z - \sigma_n^2(\mathbf{I}_M - \mathbf{E}_{op})(\mathbf{I}_M - \mathbf{E}_{op})^H. \tag{55}$$

Vectoring $\bar{\mathbf{R}}_z$ yields

$$\mathbf{r} = \mathrm{vec}(\bar{\mathbf{R}}_z) = \sum_{k=K_1+1}^{K} \bar{\mathbf{c}}_k P_k = \bar{\mathbf{C}}\mathbf{p}, \tag{56}$$

where $\bar{\mathbf{c}}_k = \mathrm{vec}(\mathbf{c}(\theta_k, \sigma_{\theta_k})\mathbf{c}^H(\theta_k, \sigma_{\theta_k}))$, $\bar{\mathbf{C}} = [\bar{\mathbf{c}}_{K_1+1}, \ldots, \bar{\mathbf{c}}_K]$, and $\mathbf{p} = [P_{K_1+1}\sigma^2_{\theta_{K_1+1}}, \ldots, P_K\sigma^2_{\theta_K}]$.

Under the sparse perturbed model, $\mathbf{r}$ can be rewritten as

$$\mathbf{r} = (\mathbf{A}' + \mathbf{F})\mathbf{p} = (\mathbf{\Phi} + \mathbf{F}_G)\mathbf{p}_G, \tag{57}$$

where $\bar{\mathbf{a}}_k = \mathrm{vec}(\mathbf{a}(\theta_k)\mathbf{a}^H(\theta_k))$, $\mathbf{A}' = [\bar{\mathbf{a}}_{K_1+1}, \ldots, \bar{\mathbf{a}}_K]$, and $\mathbf{F}$ is an $M^2 \times (K - K_1)$-dimensional perturbed matrix caused by angular spread; $\mathbf{\Phi}$, $\mathbf{F}_G$ and $\mathbf{p}_G$ are the sparse representations of $\mathbf{A}'$, $\mathbf{F}$ and $\mathbf{p}$, respectively, which are formed on a uniform grid of points describing candidate nominal DOAs $\{\theta_i\}_{i=1}^G$.

Taking the finite sample effect into account, $\mathbf{r}$ can be further expressed as

$$\mathbf{r} + \mathbf{e} = (\mathbf{\Phi} + \mathbf{F}_G)\mathbf{p}_G. \tag{58}$$

Subsequently, the S-TLS problem for perturbed model can be formulated as

$$\begin{aligned} \{\hat{\mathbf{p}}_G, \hat{\mathbf{F}}_G, \hat{\mathbf{e}}\}_{\mathrm{S-TLS}} &:= \arg \min_{\mathbf{p}_G, \mathbf{F}_G, \mathbf{e}} \|[\mathbf{F}_G \ \mathbf{e}]\|_F^2 + \varrho\|\mathbf{p}_G\|_1 \\ s.\,t.\ \mathbf{r} + \mathbf{e} &= (\mathbf{\Phi} + \mathbf{F}_G)\mathbf{p}_G, \end{aligned} \tag{59}$$

where ϱ stands for the penalty parameter.

Eliminating $\mathbf{e}$ through substituting the constraint into the cost function, (59) can be reformulated as

$$\{\hat{\mathbf{p}}_G, \hat{\mathbf{F}}_G\}_{\mathrm{S-TLS}} := \arg \min_{\mathbf{p}_G, \mathbf{F}_G} \|\mathbf{r} - (\mathbf{\Phi} + \mathbf{F}_G)\mathbf{p}_G\|_2^2 + \|\mathbf{F}_G\|_F^2 + \varrho\|\mathbf{p}_G\|_1. \tag{60}$$

Note that formulation (60) is a nonconvex problem; however, one can adopt the well-known iterative block coordinate descent algorithm [43] to transform it into two convex ones. The first convex problem at iteration i is given by

$$\mathbf{p}_G(i) = \arg \min_{\mathbf{p}_G} \|\mathbf{r} - (\mathbf{\Phi} + \mathbf{F}_G(i))\mathbf{p}_G\|_2^2 + \varrho\|\mathbf{p}_G\|_1, \tag{61}$$

which is established on the given $\mathbf{F}_G(i)$ and solved efficiently via the convex-type software package CVX [44]. With $\hat{\mathbf{p}}_G(i)$ available, the second convex problem becomes

$$\mathbf{F}_G(i+1) = \arg\min_{\mathbf{F}_G} \|\mathbf{r} - (\mathbf{\Phi} + \mathbf{F}_G)\mathbf{p}_G(i)\|_2^2 + \|\mathbf{F}_G\|_F^2, \tag{62}$$

whose closed-form solution can be easily obtained by

$$\mathbf{F}_G(i+1) = (1 + \|\mathbf{p}_G(i)\|_2^2)^{-1}[\mathbf{r} - \mathbf{\Phi}\mathbf{p}_G(i)]\mathbf{p}_G^T(i). \tag{63}$$

Run steps (61) and (63) alternately until convergence is achieved. Finally, the nominal DOAs of CD sources can be obtained by finding the indexes of $K - K_1$ non-zero peaks in $\mathbf{p}_G$.

Remark 1: Based on the convergence properties of the block coordinate descent algorithm, the solutions obtained by (61) and (63) will converge monotonically to a stationary point. On the other hand, it has been verified in [32] that the S-TLS solver can yield accurate reconstruction even with perturbations present in both $\mathbf{\Phi}$ and $\mathbf{r}$, which implies that the adopted approach is a good choice for nominal DOA estimation of CD sources. Moreover, the penalty parameter ϱ is important to guarantee the recovery performance, which can be properly selected by the L-curve method [45] or the cross-validation scheme [46].

Remark 2: One can also exploit computationally efficient approaches, such as ESPRIT [10] and unitary ESPRIT [11] for nominal DOA estimation of CD sources, which are also applicable from a theoretical point of view. However, due to influence of the oblique projection operator, the rotation invariance structure between two subarrays cannot be matched perfectly. As a result, a satisfied performance cannot be achieved, as shown later by simulation results.

3.4. Angular spread estimation

Based on the subspace theory and the nominal DOA estimates of CD sources, the angular spreads $[\sigma_{\theta_k}]_{K_1+1}^K$ associated with CD sources are estimated by

$$\hat{\sigma}_{\theta_k} = \min_{\sigma_{\theta_k}} [\mathbf{c}^H(\bar{\theta}, \sigma_\theta)\mathbf{U}_n\mathbf{U}_n^H\mathbf{c}(\bar{\theta}, \sigma_\theta)]^{-1}, \tag{64}$$

Algorithm 2 Mixed CD and ID Source Localization Approach

1: Calculate the covariance matrix $\hat{\mathbf{R}}$ and implement source enumeration according to Algorithm 1.

2: Perform EVD on $\hat{\mathbf{R}}$ to obtain the signal subspace $\hat{\mathbf{E}}_s$, and further partition it into $\hat{\mathbf{E}}_{s1}$ and $\hat{\mathbf{E}}_{s2}$.

3: Construct $\hat{\boldsymbol{\Xi}}(\theta)$ according to (46), and then obtain the nominal DOA estimation of ID sources from (51).

4: Form the oblique projection matrix $\mathbf{E}_{op}$ after reconstructing $\boldsymbol{\Gamma}$.

5: Obtain $\mathbf{z}(t)$ and covariance matrix $\hat{\mathbf{R}}_z = \frac{1}{N}\sum_{t=1}^{N}\mathbf{z}(t)\mathbf{z}^H(t)$.

6: Construct $\bar{\mathbf{R}}_z$ and further vectorize it to obtain $\mathbf{r}$ and $\boldsymbol{\Phi}$.

7: Initialize with $\mathbf{F}_G(0) = \mathbf{0}_{M^2\times G}$

for $i = 0, 1, \ldots, \kappa$ **do**

Update $\mathbf{p}_G(i)$ via (61).

Update $\mathbf{F}_G(i+1)$ as in (63).

end for

8: Obtain nominal DOAs of CD sources by finding the indexes of non-zero peaks in $\mathbf{p}_G$.

9: Estimate $[\hat{\sigma}_{\theta_k}]_{k=K_1+1}^{K}$ via (64).

10: Reconstruct $\hat{\boldsymbol{\Lambda}}$ by (65), and then estimate $[\hat{\sigma}_{\theta_k}]_{k=1}^{K_1}$ via (66).

where $\mathbf{U}_n$ is the noise subspace matrix of $\mathbf{R}_z$ or $\bar{\mathbf{R}}_z$.

With all estimated nominal DOAs and angular spreads of CD sources, $\hat{\boldsymbol{\Lambda}}$ is calculated by

$$\hat{\boldsymbol{\Lambda}} = \hat{\mathbf{D}}^{\dagger}(\hat{\mathbf{R}} - \hat{\sigma}_n\mathbf{I}_M)(\hat{\mathbf{D}}^H)^{\dagger}, \tag{65}$$

where $\hat{\mathbf{D}} = [\hat{\mathbf{A}}, \hat{\mathbf{B}}, \hat{\mathbf{C}}]$ is the estimation of GAM, $\hat{\sigma}_n$ is the average of the $M-K-K_1$ smallest eigenvalues of $\hat{\mathbf{R}}$. Therefore, angular spread of ID sources according to (24) and (25) can be obtained by

$$\hat{\sigma}_{\theta_k} = \sqrt{\frac{[\hat{\boldsymbol{\Lambda}}]_{2k,2k}}{[\hat{\boldsymbol{\Lambda}}]_{2k-1,2k-1}}}, \quad k = 1, 2, \ldots, K_1, \tag{66}$$

The proposed mixed CD and ID source localization method is summarized in Algorithm 2.

4. Discussion and Cramér-Rao Bound

4.1. Discussion

The proposed solution is discussed from four different aspects, i.e., maximum number of detectable sources, estimation accuracy, computational complexity and capability for localizing distributed sources in different scenarios.

4.1.1. Maximum Number of Detectable Sources

The maximum number of detectable sources of the proposed approach is mainly affected by three operations: i) source enumeration; 2) nominal DOA estimation of ID sources; 3) nominal DOA estimation of CD sources, where the required number of sensors satisfies $\bar{M} - 2 \geq K$, $M \geq K + K_1$ and $M \geq K_2$, respectively. By conducting simple intersection operation, we can easily conclude that $\bar{M} - 2 \geq K$. In other words, the proposed method can detect $K = \bar{M} - 2$ mixed distributed sources using a ULA of M sensors.

4.1.2. Estimation Accuracy

In general, the DOA estimation accuracy of the associated methods increases as the number of sensors, the number of snapshots and signal-to-noise ratio (SNR) increase. Except for these parameters, the performance of the proposed approach is also affected by the angular spread. For ID sources, a first-order Taylor expansion of the array manifold is used. When angular spread is sufficiently small, the GAM will be a good approximation to the true array manifold, and thus a satisfactory nominal DOA estimation performance will be provided. However, with the increase of angular spread, its estimation accuracy will degrade due to model mismatch. For CD sources, a first-order Taylor approximation is also utilized, which implies that the estimation accuracy decreases as the angular spread increases. On the other hand, the S-TLS algorithm is adopted. According the stable recovery theory [47], the mean square error (MSE) of $\hat{\mathbf{p}}_G$ is proportional to $\|\mathbf{F}_G\|_F^2$, and if angular spread is small enough, $\|\mathbf{F}_G\|_F^2$ will be small and a good nominal DOA estimation result will be obtained; otherwise, the performance will

degrade. As a result, the proposed approach is more suitable for mixed source localization with small angular spread, which is consistent with most of the existing methods for dealing with distributed source localization.

4.1.3. Computational Complexity

Regarding the computational complexity, we consider the major part, including covariance matrix construction, EVD, and the sparse recovery process. The proposed approach constructs two $M \times M$-dimensional covariance matrices and implement their EVDs. In addition, sparse recovery is performed iteratively I_t times under G spatial grids. Therefore, the resulting number of multiplications required for the proposed method is in order of $O\{2M^2N + \frac{8}{3}M^3 + I_tG^3]\}$, which is higher than that of the ESPRIT [10], [22] and the beamspace [25] based methods (whose main complexity is $O\{M^2N + \frac{4}{3}M^3\}$). However, the proposed method is a general one and can provide an improved estimation accuracy.

4.1.4. Capability for Localizing Distributed Sources

From the procedure of the proposed method, it can be seen that our method is suitable for *any* types of distributed sources. In detail, when $\hat{K}_2 = 0$, the sources are all ID, and the proposed method will reduce to the rank-reduction based method; when $\hat{K}_1 = 0$, the sources are all CD, and the proposed one will reduce to the S-TLS method. Moreover, As explained in the Section 3.2, the rank-deficiency feature of $\mathbf{\Xi}(\theta)$ only holds for nominal DOA of ID sources, which implies that only ID sources will exhibit peaks from the spatial spectrum function (51) even if some of ID and CD sources have same DOAs. On the other hand, due to the application of the oblique projection operator, the signal part of $\mathbf{z}(t)$ only contains the information of CD sources, which means that the subsequent S-TLS problem only yields DOA estimation of CD sources regardless of whether ID and CD sources have same DOAs. That is, the proposed method is also capable of mixed distributed sources localization where some of CD and ID sources have the same nominal DOAs, as shown later by computer simulations.

4.2. Approximate Cramér-Rao Bound

So far, the Cramér-Rao Bound (CRBs) for localization of distributed sources are all established on pure ID or pure CD sources. In this section, we derive the approximate CRB for the considered problem where ID and CD sources coexist. Consider the unknown parameters vector $\boldsymbol{\xi} = [\boldsymbol{\mu}^T, \boldsymbol{\nu}^T]^T$, where $\boldsymbol{\mu} = [\boldsymbol{\theta}^T, \boldsymbol{\sigma_\theta}^T]^T = [\theta_1, \ldots, \theta_K, \sigma_{\theta_1}, \ldots, \sigma_{\theta_K}]^T$ is the parameters of interest, and $\boldsymbol{\nu} = [\mathbf{P}^T, \sigma_n^2]^T = [p_1, \ldots, p_K, \sigma_n^2]^T$ is the remaining parameters. Under the condition of large N_k and small angular spread, the array covariance matrix $\mathbf{R}$ can be approximately expressed as [48]

$$\mathbf{R} \approx \sum_{k=1}^{K_1} p_k \mathbf{R}_i(\theta, \sigma_\theta) + \sum_{k=K_1+1}^{K} p_k \mathbf{R}_c(\theta, \sigma_\theta) + \sigma_n^2 \mathbf{I}_M, \tag{67}$$

where

$$\mathbf{R}_i = \mathbf{a}(\theta_k)\mathbf{a}^H(\theta_k) \odot \mathbf{G}_i(\theta_k, \sigma_{\theta_k}), \tag{68}$$

$$\mathbf{R}_c = \mathbf{c}(\theta_k, \sigma_{\theta_k})\mathbf{c}^H(\theta_k, \sigma_{\theta_k}), \tag{69}$$

and $\mathbf{G}_i(\theta_k, \sigma_{\theta_k})$ is a matrix, whose (p, q)th elements is

$$[\mathbf{G}_i(\theta_k, \sigma_{\theta_k})]_{p,q} = \begin{cases} \operatorname{sinc}(\frac{2\sqrt{3}\bar{x}_{p,q}\cos\theta_k\sigma_k}{\lambda}), \text{ uniform,} \\ \exp\left\{-\frac{(u\bar{x}_{p,q}\cos\theta_k\sigma_{\theta_k})^2}{2}\right\}, \text{Gaussian.} \end{cases} \tag{70}$$

where $\bar{x}_{p,q} = (x_p - x_q), p, q \in [1, M]$. Such an approximation is widely used in literature [22], [48], which is a convenient way to derive an appropriate CRB.

The CRB of $\boldsymbol{\xi}$ can be calculated by

$$\text{CRB}(\boldsymbol{\xi}) = \frac{1}{N}\left[\left(\frac{\partial \mathbf{r}}{\partial \boldsymbol{\xi}^T}\right)^H (\mathbf{R}^{-T} \otimes \mathbf{R}^{-1}) \frac{\partial \mathbf{r}}{\partial \boldsymbol{\xi}^T}\right]^{-1}, \tag{71}$$

where

$$\mathbf{r} = \mathbf{r}_i + \mathbf{r}_c + \sigma_n^2 \cdot \text{vec}(\mathbf{I}_M) \tag{72}$$

$$\mathbf{r}_i = \sum_{k=1}^{K_1} [p_k \mathbf{a}^*(\theta_k) \otimes \mathbf{a}(\theta_k)] \odot \text{vec}(\mathbf{G}_i(\theta_k, \sigma_{\theta_k})), \tag{73}$$

$$\mathbf{r}_c = \sum_{k=K_1+1}^{K} p_k [\mathbf{c}^*(\theta_k, \sigma_{\theta_k}) \otimes \mathbf{c}(\theta_k, \sigma_{\theta_k})]. \tag{74}$$

Through partitioning, we have

$$(\mathbf{R}^{-T/2} \otimes \mathbf{R}^{-1/2}) \left[\frac{\partial \mathbf{r}}{\partial \boldsymbol{\mu}^T} \quad \frac{\partial \mathbf{r}}{\partial \boldsymbol{\nu}^T} \right] \overset{def}{=} [\mathbf{W} \quad \mathbf{V}], \tag{75}$$

where the lth column of $\mathbf{W}$ and $\mathbf{V}$ are respectively given by

$$[\mathbf{W}(:,l)]_{l=1}^{K_1} = (\mathbf{R}^{-T} \otimes \mathbf{R}^{-1}) \frac{\partial \mathbf{r}_i}{\partial \theta_{k_1}}, \tag{76}$$

$$[\mathbf{W}(:,l)]_{l=K_1+1}^{K} = (\mathbf{R}^{-T} \otimes \mathbf{R}^{-1}) \frac{\partial \mathbf{r}_c}{\partial \theta_{k_2}}, \tag{77}$$

$$[\mathbf{W}(:,l)]_{l=K+1}^{K+K_1} = (\mathbf{R}^{-T} \otimes \mathbf{R}^{-1}) \frac{\partial \mathbf{r}_i}{\partial \sigma_{\theta_{k_1}}}, \tag{78}$$

$$[\mathbf{W}(:,l)]_{l=K+K_1+1}^{2K} = (\mathbf{R}^{-T} \otimes \mathbf{R}^{-1}) \frac{\partial \mathbf{r}_c}{\partial \sigma_{\theta_{k_2}}}, \tag{79}$$

$$[\mathbf{V}(:,l)]_{l=1}^{K} = (\mathbf{R}^{-T} \otimes \mathbf{R}^{-1}) \cdot \mathrm{vec}(\mathbf{I}_M), \tag{80}$$

$$[\mathbf{V}(:,l)]_{l=K+1}^{2K} = \mathrm{vec}(\mathbf{R}^{-1}), \tag{81}$$

where $k_1 = 1, \ldots, K_1, k_2 = K_1 + 1, \ldots, K$.

Subsequently, we can obtain

$$\mathrm{CRB}^{-1}(\boldsymbol{\xi}) = N \begin{bmatrix} \mathbf{W}^H\mathbf{W} & \mathbf{W}^H\mathbf{V} \\ \mathbf{V}^H\mathbf{W} & \mathbf{V}^H\mathbf{V} \end{bmatrix}. \tag{82}$$

Based on (82), the CRB concerning the parameters of interest is finally obtained via

$$\mathrm{CRB}(\boldsymbol{\mu}) = \frac{1}{N} \left[\mathbf{W}^H \boldsymbol{\Pi}_V^{\perp} \mathbf{W} \right]^{-1}, \tag{83}$$

where $\boldsymbol{\Pi}_V^{\perp} = \mathbf{I} - \mathbf{V}(\mathbf{V}^H\mathbf{V})^{-1}\mathbf{V}^H$.

5. Numerical Simulations

In this section, numerical simulations are carried out to evaluate the performance of the proposed method. The ESPRIT [22], the beampsace [25] based methods for ID sources, the DRNC-MUSIC [9] with known angular spread and the ESPRIT method [10] for CD sources are selected for comparison.

Additionally, the approximate CRB for the considered scenarios is also calculated for comparison. In the simulations, all the incident signals are assumed to be of equal power and binary phase shift keying (BPSK) modulated, and the variance of the ray gain and the number of paths are fixed at $\sigma_{\gamma_k} = 1$ and $[N_k]_{k=1}^K = 50$, respectively. The search step for the 1-D spectral search of (51) is 0.1°, the spatial grids for S-TLS method are initialized with 1° interval in the range of $-90°$ to 90° , and then refined with 0.1° interval around the estimated angles. In addition, the PDF of angular spread is Gaussian, and the SNR is defined as $\text{SNR} = 10\log_{10}(p_k/\sigma_n^2)$. The root mean square error (RMSE) obtained by 500 Monte-Carlo trials is used to measure the performance of the proposed method, which is defined as

$$\text{RMSE} = \sqrt{\frac{1}{500K}\sum_{k=1}^{K}\sum_{c=1}^{500}(\hat{\beta}_{k,c} - \beta_k)^2}, \tag{84}$$

where $\hat{\beta}_{k,c}$ is the estimate of β_k in the cth simulation.

In the first simulation, the normalized spatial spectrum output is presented by the proposed approach, where four scenarios are considered. *Scenario 1*: Two pure CD sources with nominal DOAs $\theta_1 = -10°$ and $\theta_2 = 15°$; *Scenario 2*: Two pure ID sources with nominal DOAs $\theta_1 = -10°$ and $\theta_2 = 15°$; *Scenario 3*: One ID source with nominal DOA $\theta_1 = -10°$, and two CD sources with nominal DOAs $\theta_2 = 10°$ and $\theta_3 = 20°$; *Scenario 4*: One ID source with nominal DOA $\theta_1 = -10°$ and two CD sources with nominal DOAs $\theta_2 = -10°$ and $\theta_3 = 20°$. All the angular spreads are fixed at $\sigma_\theta = 1.5°$; the number of sensors M, the number of snapshots N and SNR are set to 10, 200 and 15 dB, respectively. It can be seen from Fig. 2 that the proposed method is not only suitable for dealing with pure CD and ID sources, but also mixed CD and ID sources. Meanwhile, it also works for mixed source localization where some of CD and ID sources have the same nominal DOAs.

In the second simulation, the source enumeration performance of the proposed method is examined, whose probability of correct detection curves at different SNRs, different number of sensors and snapshots are shown in Fig. 3. The probability of correct detection is defined as $P_c = I_c/500$, where I_c stands for the number of correct source enumerations in 500 independent Monte-Carlo trials. One ID source and

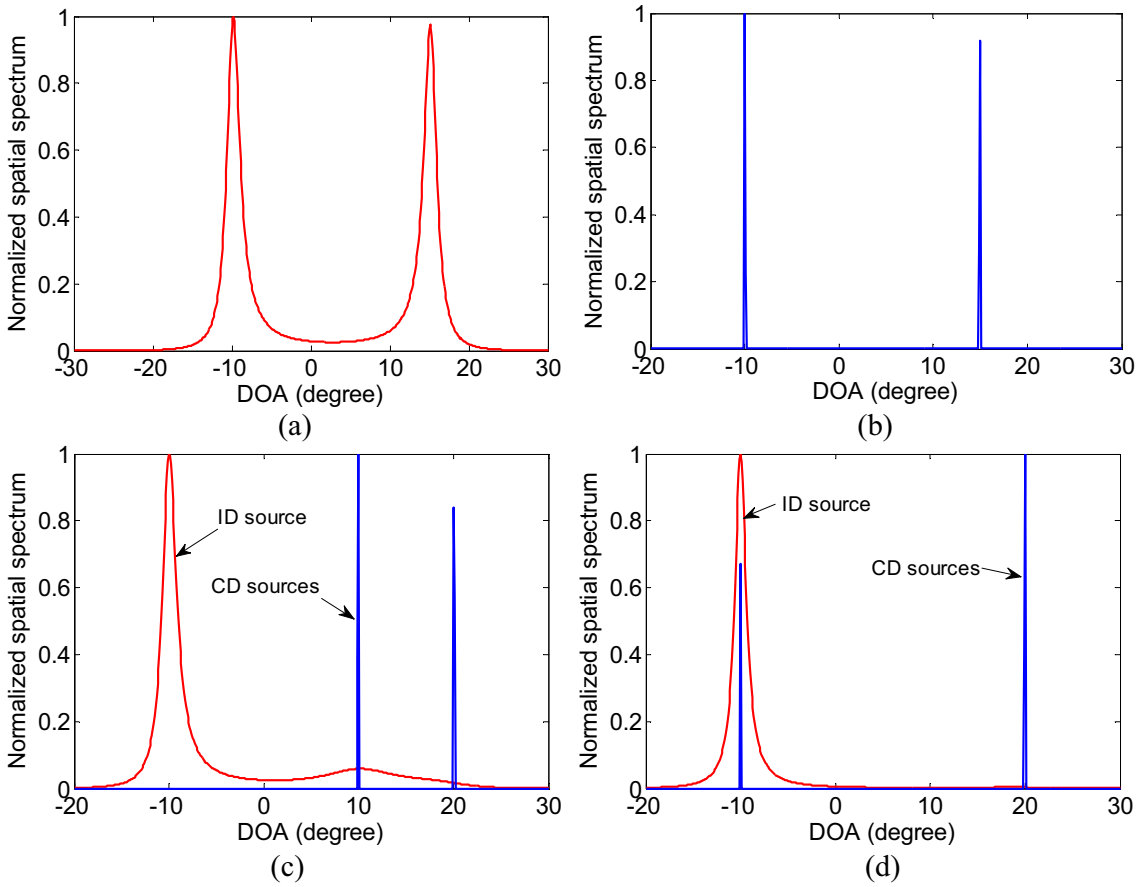

Figure 2: Normalized spatial spectrum obtained by the proposed approach, $M = 10$, $N = 200$, SNR=15 dB, and $\sigma_\theta = 1.5°$. (a) Two CD sources with $\theta_1 = -10°$, $\theta_2 = 15°$. (b) Two ID sources with $\theta_1 = -10°$, $\theta_2 = 15°$. (c) One ID source with $\theta_1 = -10°$ and two CD sources with $\theta_2 = 10°$, $\theta_3 = 20°$. (d) One ID source with $\theta_1 = -10°$ and two CD sources with $\theta_2 = -10°$, $\theta_3 = 20°$.

one CD source with their parameters $\{\theta_1 = -10°, \sigma_{\theta_1} = 1°\}$ and $\{\theta_2 = 15°, \sigma_{\theta_2} = 1°\}$ are considered. In Fig. 3(a), SNR is fixed at 10 dB, whereas M varies from 10 to 20 and N from 50 to 150. In Fig. 3(b), N is fixed at 100, and M varies from 10 to 20 and SNR from 8 dB to 12 dB. From the simulation result, we can observe that the proposed method can provide an effective source number estimation result. In particular, when $M \geq 12$, $N \geq 100$ and SNR$\geq$ 10 dB, the probability of correct detection is higher than 90%. Based on this simulation, and also for the sake of simplicity, we assume that the number of sources has been correctly estimated in subsequent simulations.

In the third simulation, the performance is evaluated with respect to SNR. The parameters of two incident signals for the proposed method are the same as in the second simulation. For reasonable

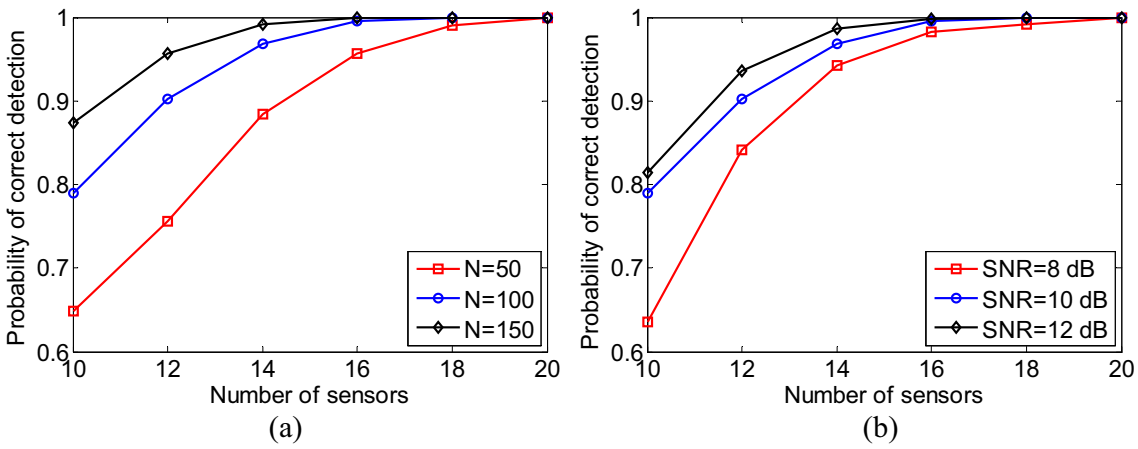

Figure 3: Probability of correct detection by the proposed source enumeration scheme for one ID source with $\theta_1 = -10°$ and one CD source with $\theta_2 = 15°$, $\sigma_{\theta_{k_1}} = \sigma_{\theta_{k_2}} = 1°$. (a) Different number of sensors and snapshots. (b) Different SNRs and number of sensors.

comparison, two ID sources (whose location information is the same as that of the proposed one) are considered for the ESPRIT [22] and beamspace [25] based methods, since they cannot deal with mixed distributed sources. Once the nominal DOA of ID sources is estimated and the component of ID sources is eliminated by oblique projection, the DRNC-MUSIC [9] and ESPRIT [10] based solutions proposed for CD sources are also employed for comparison. The simulation result with $M = 12$ and $N = 200$ is shown in Fig. 4. It can be seen that the proposed one outperforms the other methods for nominal DOA estimation of both ID and CD sources in the whole SNR region. For angular spread estimation of ID sources, the proposed method performs better than the beamspace method, and also better than the ESPRIT method [22] when SNR$\leq$8 dB. For angular spread estimation of CD sources, the new method again provides a lower RMSE than the ESPRIT method in [10].

In the fourth simulation, the performance of the proposed method is examined for different number of snapshots N, and the results are shown in Fig. 5. The simulation configuration is the same as in the third simulation, except that SNR is fixed at 8 dB, while N varies from 50 to 300 in a step of 50. From Fig. 5, it can be seen that the RMSE of all methods decreases as N increases, and again the proposed one outperforms the compared ones. In addition, it can be seen from Fig. 5(a) that there is a clear gap

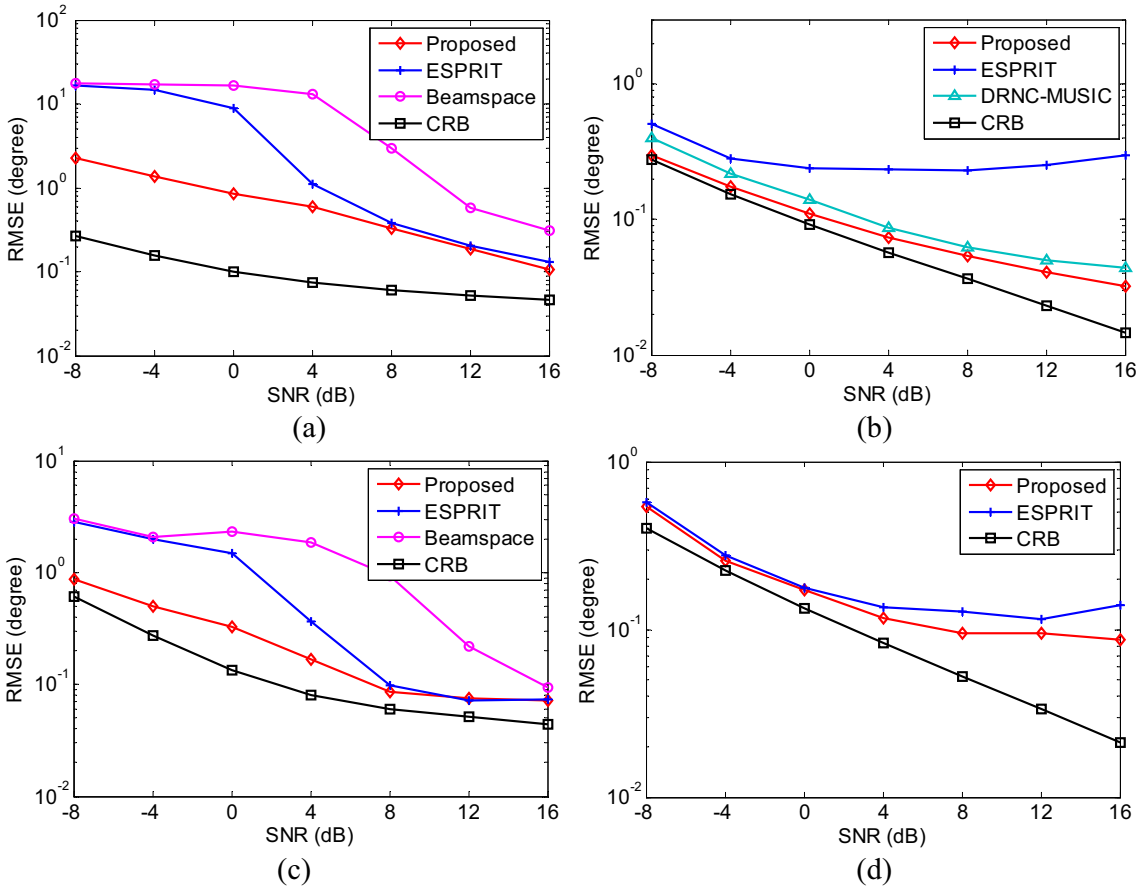

Figure 4: RMSE of nominal DOA and angular spread estimation with respect to SNR, with $M = 12$, $N = 200$, $\theta_1 = -10°$, $\theta_2 = 15°$, and $\sigma_{\theta_1} = \sigma_{\theta_2} = 1°$. (a) Nominal DOA estimation of ID sources. (b) Nominal DOA estimation of CD sources. (c) Angular spread estimation of ID sources. (d) Angular spread estimation of CD sources.

between the RMSEs of the proposed method and the CRB. This can be explained as follows: For the nominal DOA estimator of ID sources, it can be regarded as a pure ID source localization problem in the presence of CD source interference, and such an interference directly yields that the RMSE of the proposed method cannot follow the CRB well.

In the fifth simulation, the performance is studied for different values of sensor number M. The simulation conditions are again the same as in the third simulation, except that the SNR is fixed at 8 dB, and M varies from 10 to 20. Fig. 6 shows the RMSEs of the nominal DOA and angular spread estimates versus M, where the performance of the proposed method improves as M increases, and its trend matches well with that of the CRB. As a comparison, the performance of the ESPRIT method

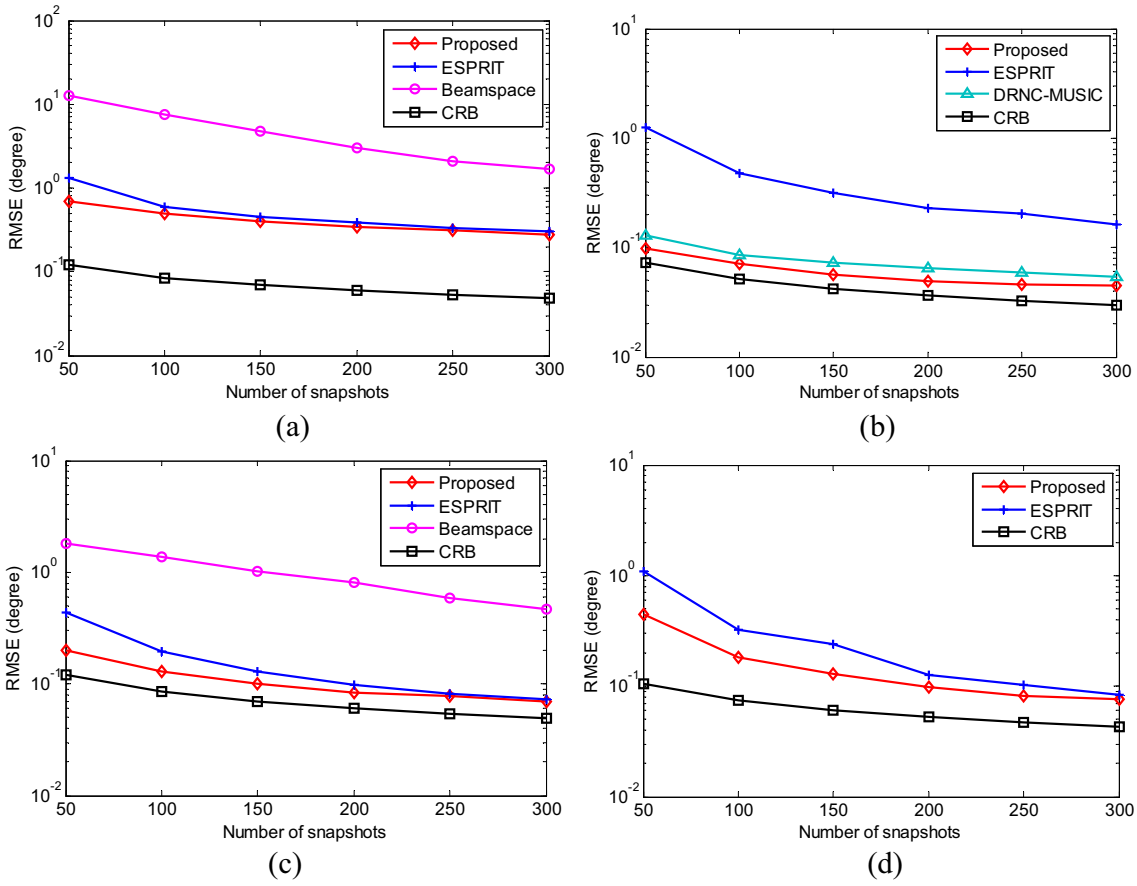

Figure 5: RMSE of nominal DOA and angular spread estimation for different number of snapshots, with $M = 12$, SNR=8 dB, $\theta_1 = -10°$, $\theta_2 = 15°$, and $\sigma_{\theta_1} = \sigma_{\theta_2} = 1°$. (a) Nominal DOA estimation of ID sources. (b) Nominal DOA estimation of CD sources. (c) Angular spread estimation of ID sources. (d) Angular spread estimation of CD sources.

[10] for nominal DOA estimation of CD sources, as well as other compared methods for angular spread estimation degrades as M increases in certain ranges of the number of sensors. Such a phenomenon can be explained as follows. We have clarified that the ESPRIT method proposed for CD sources in [10] is employed for comparison after eliminating the components of ID sources by the oblique projection technique. However, due to the limited number of snapshots and application of the oblique projection operator, there will be perturbations in the observation model $\mathbf{z}(t)$, resulting in the rotation-invariant structure between two subarrays not being perfectly maintained. In particular, the impact of such perturbations may increase with the increase of M and SNR, especially for a relatively small number of snapshots. As a result, the RMSEs of the relevant parameters of the ESPRIT method increase, as

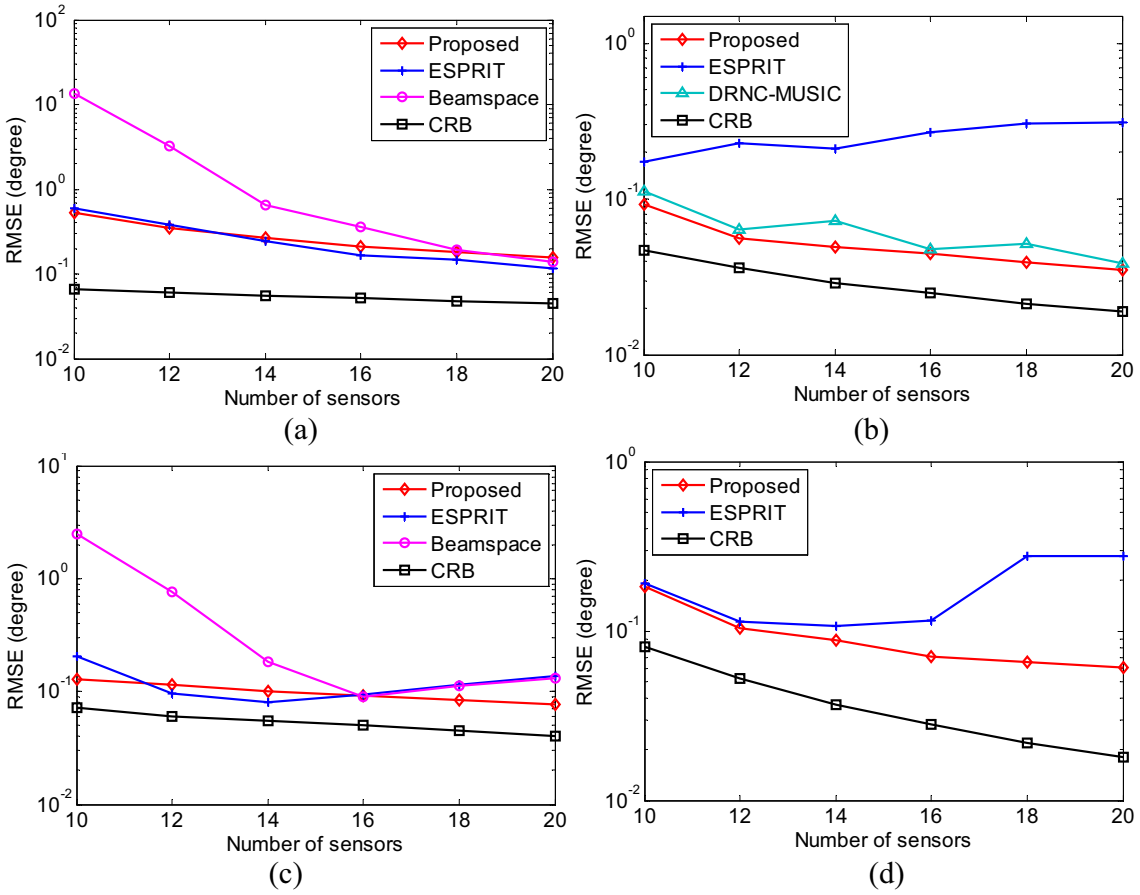

Figure 6: RMSE of nominal DOA and angular spread estimation for different number of sensors, with $N = 200$, SNR=8 dB, $\theta_1 = -10°$, $\theta_2 = 15°$, and $\sigma_{\theta_1} = \sigma_{\theta_2} = 1°$. (a) Nominal DOA estimation of ID sources. (b) Nominal DOA estimation of CD sources. (c) Angular spread estimation of ID sources. (d) Angular spread estimation of CD sources.

shown in Figs. 6(b) and 6(d) (also shown in Figs. 4(b) and 4(d)). In addition, also affected by the limited number of snapshots, the estimation performance for angular spreads by the beamspace based method also decreases as M increases to a certain extent, which coincides with the results in Fig. 3(d) of [25].

In the sixth simulation, the performance is tested for different angle separations. M, N and SNR are set to 12, 200 and 4 dB, respectively. The nominal DOA θ_1 of one ID source is fixed at $-10°$, whereas that θ_2 of one CD source is changed from $-4°$ to $11°$ in a step of $3°$, with $\sigma_{\theta_1} = \sigma_{\theta_2} = 1°$. The RMSE curves are shown in Fig. 7, from which we can see that the performance of all estimators improves with the increase of angle separation. Moreover, it can be further observed that the proposed method can

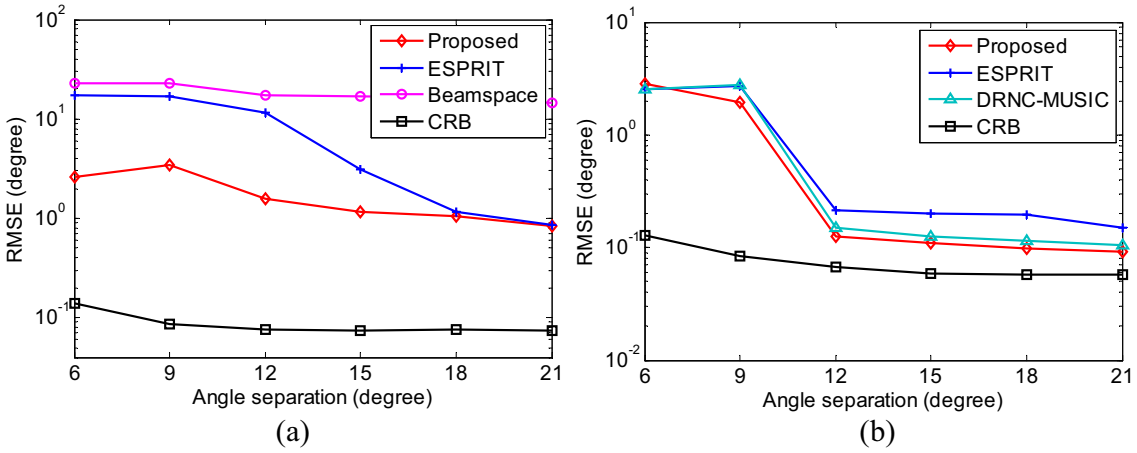

Figure 7: RMSE of nominal DOA estimation versus angle separation, with $M = 20$, $N = 200$ and SNR=4 dB. (a) Nominal DOA estimation of ID sources. (b) Nominal DOA estimation of CD sources.

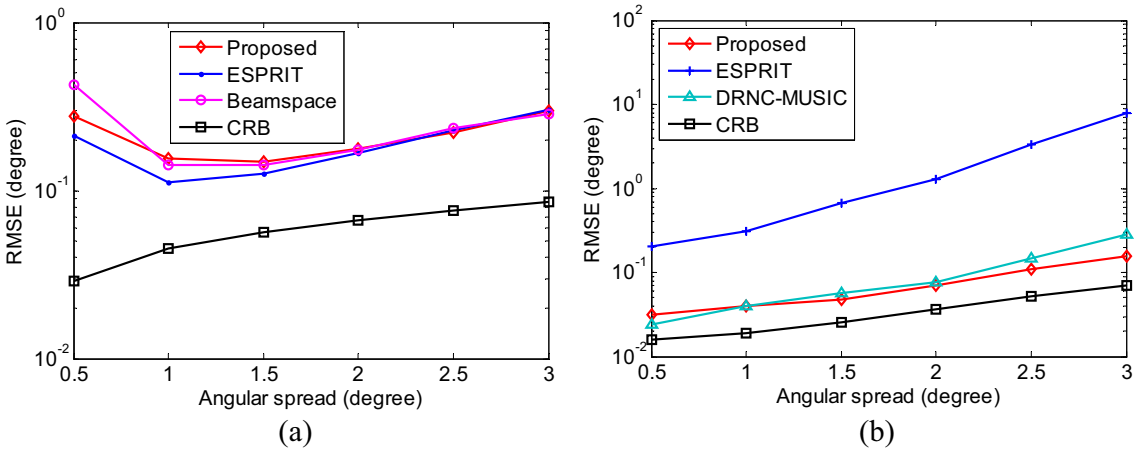

Figure 8: RMSE of nominal DOA estimation versus angular spread, with $M = 20$, $N = 200$, SNR=8 dB, and $\theta_1 = -10°$, $\theta_2 = 15°$. (a) Nominal DOA estimation of ID sources. (b) Nominal DOA estimation of CD sources.

obtain a good estimate when angle separation is greater than 9°, showing its robustness against closely spaced sources compared with other methods.

In the seventh simulation, the performance of the proposed method is assessed with respect to angular spread. M, N and SNR are set to 20, 200 and 8 dB, respectively. One ID source with nominal DOA $\theta_1 = -10°$, and one CD source with nominal DOA $\theta_2 = 15°$ are considered, and the angular spreads of two sources are equal and vary from 0.5 to 3. As can be seen in Fig. 8, for CD sources, the RMSE of nominal DOA estimation of the proposed method decreases with the increase of angular spread, while

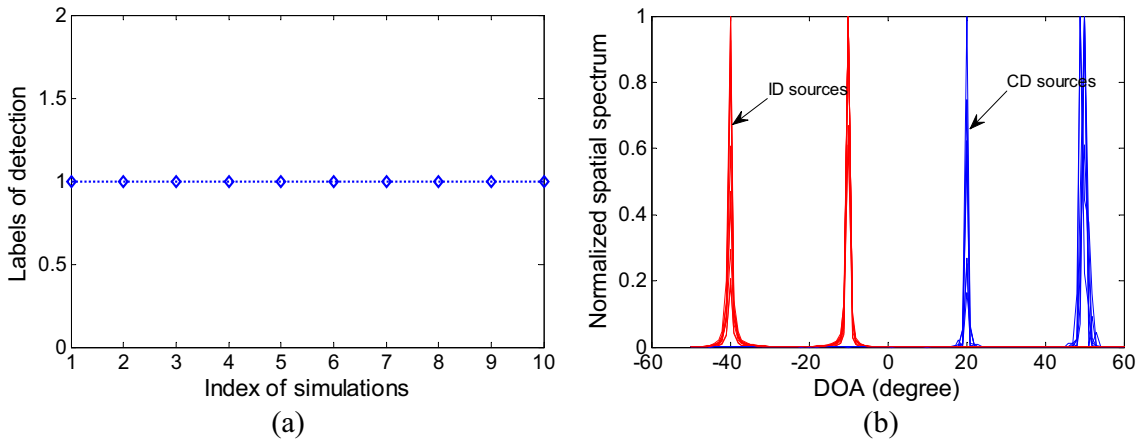

Figure 9: Validation of maximum number of detectable sources for the proposed method, with $M = 12$, $N = 200$, and SNR=20 dB, two ID sources from $\theta_1 = -40°$ and $\theta_2 = -10°$, and two CD sources from $\theta_3 = 20°$ and $\theta_4 = 50°$. (a) Result of source enumeration; (b) normalized spatial spectrum.

for ID sources, the overall trend of nominal DOA estimation of all methods goes up as the angular spread increases, provided that angular spread is larger than 1°, which is consistent with the discussion in Section IV. On the other hand, it is necessary to point out here that the performance of the proposed method is also affected by other parameters, and when the angular spreads of ID sources are rather small, the expectations of the diagonal elements of $\hat{\mathbf{\Lambda}}$ formulated in (19) are small. Thus, the impact of noise becomes the dominant factor, which finally yields that the RMSE of nominal DOA estimation of ID sources decreases as the angular spread increases, when angular spread is smaller than roughly 1°.

In the last simulation, we further validate the capacity of the proposed method in terms of the maximum number of detectable sources. Four distributed sources containing two ID sources from $\theta_1 = -40°$ and $\theta_2 = -10°$, and two CD sources from $\theta_3 = 20°$ and $\theta_4 = 50°$ are considered with $M = 12$, $N = 200$, SNR=20 dB, and $\sigma_{\theta_k} = 1°, k = 1, 2, 3, 4$. A value of one is used to indicate that the number of sources has been correctly detected in the pth simulation, where $p \in [1, 10]$; otherwise, it is zero. As can be seen in Fig. 9, the proposed method can detect $\bar{M} - 2 = 4$ distributed sources successfully using a ULA of $M = 12$ sensors, which is consistent with the analysis in Section 4.1.1.

6. Conclusion

In this paper, a novel source localization method for mixed ID and CD sources has been proposed based on the GAM under the small angular spread assumption. As a general solution, it can be applied for localization of different types of distributed sources. First, an efficient source enumeration scheme was developed, suitable for number estimation of mixed CD and ID sources as well as classification of source types. With the aid of source enumeration result, the rank-reduction principle based 1-D spectral search and the S-TLS method were respectively exploited for nominal DOA estimation of ID and CD sources. Numerical simulations show that the proposed method has outperformed some representative methods considered, and more importantly none of those existing methods can deal with the most general case of the problem.

Acknowledgement

This work was supported in part by Zhejiang Provincial Natural Science Foundation of China under Grants LY23F010004, LY23F010003, and in part by the the National Natural Science Foundation of China (NSFC) under Grants 62001256, 61871246.

[1] H. Xie, F. Gao, S. Zhang, and S. Jin, A unified transmission strategy for TDD/FDD massive MIMO systems with spatial basis expansion model, IEEE Trans. Veh. Technol. 66 (4) (2017) 3170–3184.

[2] P. Hu, X. Su, and Z. Liu, Direction finding for passive bistatic radar in the presence of multipath propagation, Wireless Commun. Mobile Comput. (2022) 7562517.

[3] Z. Liu, J. Wu, S. Yang, and W. Lu, DOA estimation method based on EMD and MUSIC for mutual interference in FMCW automotive radars, IEEE Geosci. Remote Sens. Lett. 19 (2022) 1–5.

[4] Y. Ning, S. Ma, F. Meng, and Q. Wu, DOA estimation based on ESPRIT algorithm method for frequency scanning LWA, IEEE Commun. Lett. 24 (7) (2020) 1441–1445.

[5] M. Fu, Z. Zheng and W. -Q. Wang, 2-D DOA estimation for nested conformal arrays via sparse reconstruction, IEEE Commun. Lett. 25 (3) (2021) 980–984.

[6] R. Shafin, L. Liu, J. Zhang, and Y. C. Wu, DOA estimation and capacity analysis for 3-D millimeter wave massive-MIMO/FD-MIMO OFDM systems, IEEE Trans. Wireless Commun. 15 (10) (2016) 6963–6978.

[7] R. Cao, F. Gao, and X. Zhang, An angular parameter estimation method for incoherently distributed sources via generalized shift invariance, IEEE Trans. Signal Process. 64 (17) (2016) 4493–4502.

[8] S. Valaee, B. Champagne, and P. Kabal, Parametric localization of distributed sources, IEEE Trans. Signal. Process. 43 (9) (1995) 2144–2153.

[9] L. Wan, G. Han, and J. Jiang, DOA estimation for coherently distributed sources considering circular and noncircular signals in massive MIMO systems, IEEE Syst. J. 11 (1) (2017) 41–49.

[10] S. Shahbazpanahi, S. Valaee, and M. H. Bastani, Distributed source localization using ESPRIT algorithm, IEEE Trans. Signal. Process. 49 (10) (2001) 2169–2178.

[11] Y. Zhou, Z. Fei, S. Yang, J. Kuang, S. Chen, and L. Hanzo, Joint angle estimation and signal reconstruction for coherently distributed sources in massive MIMO systems based on 2-D unitary ESPRIT, IEEE Access 5 (2017) 9632–9646.

[12] X. Yang, G. Li, and Z. Zheng, Low-complexity 2D DOA estimator of coherently distributed non-circular sources, in Proc. Int. Conf. Wireless Commun. Signal Process. Hangzhou, China, Oct. 2013, pp. 1-5.

[13] Z. Zheng, G. Li, and Y. Teng, 2D DOA estimator for multiple coherently distributed sources using modified propagator, Circuit Syst. Signal Process. 31 (1) (2010) 255–270.

[14] Y. Han, J. Wang, X. Song, and Y. Zhang, Joint estimation of central direction of arrival and angular spread for distributed source based on beamspace propagator, in Proc. 6th World Cong. Intel. Control and Auto.Dalian, China, Jun. 2006, pp. 1693-1696.

[15] A. Zoubir and Y. Wang, Performance analysis of the generalized beamforming estimators in the case of coherently distributed sources, Signal Process. 88 (2) (2008) 428–435.

[16] F. Liu, K. Tang, Z. Su, R. Du, and A. Zhang, LP-DSPE algorithm for angular parameter estimation of coherently distributed sources, IEEE Commun. Lett. 26 (1) (2022) 79–83.

[17] Y. Tian, H. Yue, and X, Rong, Multi-parameters estimation for coherently distributed sources under coexistence of circular and noncircular signals, IEEE Commun. Lett. 24 (6) (2020) 1254–1257.

[18] Y. Meng, P. Stoica, and K. Wong, Estimation of the directions of arrival of spatially dispersed signals in array processing, in Proc. IEE Radar, Sonar Navigat. Feb. 1996, vol. 143, no. 1, pp. 1-9.

[19] O. Besson and P. Stoica, Decoupled estimation of DOA and angular spread for a spatially distributed source, IEEE Trans. Signal Process. 48 (7) (2000) 1872–1882.

[20] M. Bengtsson and B. Ottersten, A generalization of weighted subspace fitting to full-rank models, IEEE Trans. Signal Process. 49 (5) (2001) 1002–1012.

[21] M. Bengtsson and B. Ottersten, Rooting techniques for estimation of angular spread with an antenna array, in Proc. IEEE Veh. Technol. Conf., Phoenix, AZ, USA, May 1997, vol. 2, pp. 1158-1162.

[22] A. Hu, T. Lv, H. Gao, Z. Zhang, and S. Yang, An ESPRIT-based approach for 2-D localization of incoherently distributed sources in massive MIMO systems, IEEE J. Sel. Topics Signal Process. 8 (5) (2014) 996–1011.

[23] Y. Tian, W. Liu, H. Xu, S. Liu, and Z. Dong, 2-D DOA estimation of incoherently distribut-

ed sources considering gain-phase perturbations in massive MIMO systems, IEEE Trans. Wireless Commun. 21 (2) (2022) 1143–1155.

[24] Q. Gu, H. Wang, W. Sun, T. Wu, and Y. Xu, A sequential ESPRIT algorithm based on a novel UCSA configuration for parameteric estimation of two-dimensional incoherently distributed source, IEEE Trans. Veh. Technol. 70 (1) (2021) 356–370.

[25] Z. Zheng, J. Lu, W. Wang, H. Yang, and S. Zhang, An efficient method for angular parameter estimation of incoherently distributed sources via beamspace shift invariance, Digital Signal Process. 83 (2018) 261–270.

[26] Z. Zheng, W. Wang, H. Meng, S. C. So, and H. Zhang, Efficient beamspace-based algorithm for two-dimensional DOA estimation of incoherently distributed sources in massive MIMO systems, IEEE Trans. Veh. Technol. 67 (12) (2018) 11776–11789.

[27] X. Yang, G. Li, Z. Zheng, C. C. Ko, and T. S. Yeo, Parameter estimation of incoherently distributed source based on block sparse Bayesian learning, in Proc. 2015 IEEE Int. Conf. Digital Signal Process. Singapore, Jul. 2015, pp. 633-637.

[28] B. T. Sieskul, An asymptotic maximum likelihood for joint estimation of nominal angles and angular spreads of multiple spatially distributed sources, IEEE Trans. Signal Process. 59 (3) (2010) 1534–1538.

[29] Y. Xiong, G. Zhang, B. Tang, and H. Cheng, Blind indentification and DOA estimation for arrays sources in the presence of scattering, J. Syst. Eng. Elec. 22 (3) (2011) 393–397.

[30] C. Li, X. Chen, and X. Liu, Cognitive tropospheric scatter communication, IEEE Trans. Signal. Process. 67 (2) (2018) 1482–1491.

[31] G. Zhang, Research on multiple dimensional parameter estimation for complicated spatial signal, Ph.D. dissertation, University of Elec. Sci. Technology of China, Xi'an, 2009.

[32] H. Zhu, G. Leus, and G. B. Giannakis, Sparsity-cognizant total least-squares for perturbed compressive sampling, IEEE Trans. Signal Process. 59 (5) (2011) 2002–2016.

[33] D. Asztely, B. Ottersten, and A.L. Swindlehurst, Generalised array manifold model for wireless communication channels with local scattering, IEE Proc. Radar. Sonar. Naving. 145 (1) (1998) 51–57.

[34] D. Astely and B. Ottersten, The effects of local scattering on direction of arrival estimation with MUSIC, IEEE Trans. Signal Process. 47 (12) (1999) 3220–3234.

[35] P. Zetterberg and B. Ottersten, The spectrum efficiency of a base station antenna array system for spatially selective transmission, IEEE Trans Veh. Technol. 44 (3) (1995) 651–660.

[36] L. Huang, T. Long, and E. Mao, MMSE-based MDL method for accurate source number estimation, IEEE Signal Process. Lett. 16 (9) (2009) 798–801.

[37] X. Ma, X. Dong, and Y. Xie, An improved spatial differencing method for DOA estimation with the coexistence of uncorrelated and coherent signals, IEEE Sensors J. 16 (10) (2016) 3719–3723.

[38] Y. Tian, X. Gao, R. Wang, Z. Dong, and H. Xu, Modified spectral function based DOA estimation in colored noise, Int. J. Electron. Commun. 138 (2021) 153892.

[39] G. Liu and X. Sun, Spatial differencing method for mixed far-field and near-field sources localization, IEEE Signal Process. Lett. 21 (11) (2014) 1331–1335.

[40] Y. Tian, X. Gao, W. Liu, and H. Chen, Phase compensation based localization of mixed far-field and near-field sources, IEEE Wireless Commun. Lett. 11 (3) (2022) 598–601.

[41] R. T. Behrens and L. L. Scharf, Signal processing applications of oblique projection operators, IEEE Trans. Signal Process. 42 (6) (1994) 1413–1424.

[42] R. Boyer and G.Bouleux, Oblique projections for direction-of-arrival estimation with prior knowledge, IEEE Trans. Signal Process. 56 (4) (2008) 1374–1387.

[43] P. Tseng, Convergence of a block coordinate descent method for nondifferentiable minimization, J. Optim. Theory Appl. 109 (3) (2001) 475–494.

[44] M. Grant and S. Boyd, CVX: MATLAB software for disciplined convex programming, April 2010, Available Online at: http://cvxr.com/cvx.

[45] P. C. Hansen and D. P. OLeary, The use of the L-curve in the regularization of discrete ill-posed problems, SIAM J. Sci. Comput. 14 (6) (1993) 1487–1503.

[46] J. Shao, Linear model selection by cross-validation, J. American Statis. Asso. 88 (422) (1993) 486–494.

[47] M. A. Herman and T. Strohmer, General deviants: An analysis of perturbations in compressed sensing, IEEE J. Sel. Topics Signal Process. 4 (2) (2010) 342–349.

[48] W. J. Bangs, Array processing with generalized beamformers, Ph. D. dissertation, Yale Univ., New Haven, CT, USA, 1971.